

## Experimental Investigation of Shell-and-Tube Heat Exchanger Performance using $Al_2O_3$ -Water Nanofluid

AL-Hussein A. Khalaf <sup>a,\*</sup>

*a. Missan Oil Company, Iraq, Alimera*

\*Corresponding author. E-mail address: [alhussen2009mh@gmail.com](mailto:alhussen2009mh@gmail.com)

Received:	10/3/2026	Accepted:	3/6/2026	Published:	28/6/2026
-----------	-----------	-----------	----------	------------	-----------

### Abstract

This paper presents a comparative study of thermal properties of a shell and tube type heat exchanger filled with an  $Al_2O_3$ -water nanofluid with the one filled by pure water. It was decided to use Aluminum oxide ( $Al_2O_3$ ) because it was chemically stable, commercially available and found to be effective in improving thermal conductivity without extreme hydraulic penalties. The experiments were carried out for a range of Reynolds numbers between [12,600 to 63,300] and at a concentration of 30g per 10L of base fluid. The effectiveness-NTU ( $\epsilon$ -NTU) approach was used for data reduction. The results indicate that the counter-flow design produced a large positive effect, increasing the effectiveness by 17-19%, and a reduction in the fluid temperature at the high end by about 5°C. The parallel-flow configuration enhanced the performance as well, with an approximate 16% more effectiveness gain. The improvement in thermal conductivity was achieved with the addition of nanoparticles; however, the increase in the fluid viscosity means that extra pumping power may be necessary. In conclusion, low concentration  $Al_2O_3$  nanofluids are potentially useful to enhance the thermal efficiency of the heat transfer processes used in industry, but hydraulic losses must be adequately reduced.

Keywords: Shell-and-tube heat exchanger; Nanofluid; Heat transfer enhancement; Effectiveness-NTU method; Counter-flow arrangement.

### 1. Introduction

The heat exchangers are important in petrochemical processing, power generation and heating, ventilation, and air conditioning studies, where the quality of heat exchangers affects the straightforward energy efficiency and reliability of the system. Of all the available configurations, shell-and-tube heat exchangers are widely used since they are mechanically robust and flexible in their operations. Although they have these benefits, their thermal performance is often constrained by the relatively low thermal conductivity of traditional heat-transfer fluids, including water. Over the last few years, the use of nanofluids has become one of the viable measures to overcome this constraint. By dispersing solids into a base fluid, the performance of the exchanger in terms of heat-transfer can be improved without altering the geometry of the exchanger, making nanofluids an attractive solution to the current systems to improve their performance. This paper compares the thermal behavior of a shell-and-Tube heat exchanger that uses an  $Al_2O_3$ -water nanofluid. Recent progress in modern materials science has enabled the synthesis of nanometer-scale particles exhibiting mechanical, thermal, and physicochemical properties that differ substantially from those of their bulk counterparts. The

utilization of such nanoparticles to tailor and enhance the thermal performance of conventional heat transfer fluids has therefore attracted significant and growing research interest. Nanofluids are defined as advanced heat transfer media consisting of solid nanoparticles, typically with characteristic dimensions below 100 nm in at least one direction, uniformly and stably dispersed within a base fluid, leading to modified thermophysical properties and improved heat transfer behavior [1]. Nanofluids are particularly well suited for advanced engineering applications and offer several advantages over conventional solid-liquid suspensions, including enhanced colloidal stability, a substantial increase in effective thermal conductivity, and negligible additional pressure drop under comparable flow conditions [2]. Nanofluids are technically defined as homogeneously dispersed colloidal suspensions of nanoparticles of solid materials, mostly with diameters below 100 nanometers, into a base fluid. Metal-oxide nanoparticles, especially aluminium oxide ( $\text{Al}_2\text{O}_3$ ) and titanium dioxide ( $\text{TiO}_2$ ), are used often due to their chemical strength, commercial accessibility, and favorable thermal properties. Empirical studies have shown time and again that nanofluids have the ability to significantly improve the performance of heat transfer by increasing the effective thermal conductivity of the working fluid [3], [4], [5]. The initial experimental studies were largely focused on simple geometries in heat exchangers, especially the use of the two pipes. A longitudinal evaluation of the heat transfer and pressure-drop properties of  $\text{TiO}_2$ -water nanofluids in a counter-flow and double-pipe heat exchanger in laminar, transitional and turbulent flow was conducted experimentally by Subramanian et al. [6]. The volume fractions of nanoparticles were tested as 0.1 % to 0.5 %, and the results showed that the heat transfer rate rose with the Reynolds number and the nanoparticle concentration with the highest percentage of about 25 % compared to pure water. However, an increase in pressure drop was also noted in the investigation due to the high viscosity of the nanofluid. Further studies later expanded the use of nanofluids into plate heat exchangers. In one example, Bozorgan and Shafahi [7] performed a numerical study of an aluminum oxide ( $\text{Al}_2\text{O}_3$ )-water nanofluid in a plate heat exchanger and found that a heat-transfer enhancement of about 12 % was obtained with only a slight increase in pumping power at an optimum nanoparticle volume fraction. Similarly, Sozen et al. [8] conducted experimental research on titanium dioxide ( $\text{TiO}_2$ ) water nanofluid in a plate heat exchanger and observed that the rate of heat-transfer increased by up to 11% as compared to plain water. All these studies have the overall implication that even the small concentrations of nanoparticles can impart significant thermal benefits with minimal hydraulic penalties. New research has also dwelt on advanced nanofluids especially including carbon-based nanomaterials. Hassaan [9] in an empirical investigation of the performance of MWCNT-laden nanofluids in a two-pipe heat exchanger system found a strong increase of the Nusselt number, up to 68% more than with distilled water. However, despite these advanced thermal transportation properties, carbon based nanofluids are limited by high cost, stability, and complexities involved in synthesis hence makes them less suitable in laboratory scale studies as compared to the metal oxide nanofluids. Regarding shell-and-tube type of heat exchangers, empirical studies have supported the ability of nanofluids to improve the heat transfer performance. Shahrul et al. [10] and Farajollahi et al. [11] obtained experimental studies of  $\text{Al}_2\text{O}_3$ -water nanofluids in shell-and-tube heat exchangers and reported significant enhancement in the heat transfer coefficient compared with pure water. However, such investigations also simultaneously highlight the fact that an increase in the concentration of nanoparticles creates pressure losses that can be detrimental to the performance of the system,

the heat-transfer system. The need to determine the performance of nanofluids using system-level parameters has been highlighted by researchers instead of using local heat transfer parameters. In their study, Hasan et al. [12] explore the creation of a new three-zonal trefoil baffle design that aims to balance the limitations between heat transfer efficiency and pressure drop in shell-and-tube heat exchangers (STHEs). This innovative design combines the flow enhancing properties of eccentric trefoil tube holes (which minimizes the area of contact between the tubes and the baffles), with three large zonal openings in 120° configuration. rotational symmetry to reduce "dead zones" and promote continuous fluid flow. The study shows that the conventional segmental baffles can offer approximately 16.67% increase in absolute heat transfer compared to the proposed design but results in a much higher pressure drop (as much as 41.46% higher than the proposed design) through a dual methodology of numerical simulation with the realizable  $k-\epsilon$  turbulence model and experimental validation. The novel baffle ended up with 13.07% enhancement in the heat transfer per unit pressure drop ( $Q/\Delta P$ ) and showed better efficiency for high flow rate systems ( $Re > 15000$ ) where the reduction of pumping power and maintenance cycles is an important operating goal. The study provides a useful reference for future baffle configurations that would further promote energy efficiency and thermal management in industrial uses like power plants and refinery. A finite element method (FEM) is used to investigate a full-scale four-tube-path shell-and-tube heat exchanger (STHx) with a high fidelity numerical simulation of the thermohydraulic performance of periodically inward corrugated (PIC) tubes by the author(s) Gao et al. [13]. The study shows that the total heat exchange rate with the use of PIC tubes can be increased by 12% to 20% over the plain tubes and this is attributed to the induction of strong secondary flows that greatly enhance the fluid mixing, which is the primary purpose of the application. This thermal enhancement results in a larger pressure drop in the tube side but the corrugated geometry allows for a more uniform mass flux distribution throughout the tube bundle, thereby helping to minimize flow maldistribution and reduce the pressure resistance on the shell side by some 14%. Interestingly, the study highlights the need for ultra-high-resolution modeling (up to 50 million grid points) to resolve detailed pressure gradients and show that pressure drops in the header, and distributor may constitute a significant fraction (up to 69.2%) of the total. The authors finally concluded that PIC tubes are most effective at low Reynolds numbers, thereby offering a solid approach to improve the compactness and efficiency of operation of complex industrial thermal systems, by providing a higher STHx. As shown by Unverdi and Kucuk [14], despite the potential advantages of the nanofluids in improving the local heat transfer, the total efficiency of shell-and-tube heat exchangers might be decreased in cases where pumping power consumption is added. This highlights the need to use holistic methods of performance assessment, including the effectiveness-NTU method. Overall, it can be affirmed that the available literature confirms that  $Al_2O_3$ -water nanofluids are promising working fluids in enhancing heat transfer in various geometries of heat-exchangers. However, the extent of improvement is significantly dependent on the concentration of nanoparticles, flow arrangement and running conditions. Moreover, there are few experimental studies which consider the traditional type of shell-to-tube heat exchangers on the laboratory scale and directly compare parallel and counter-flow systems using the effectiveness-NTU methodology. Due to the identified gaps in literature, the recent developments of optimization of heat exchangers have been directed toward synergistic effect of low concentration nanofluids applied to system-level optimization methods such as the  $\epsilon$ -NTU

method. Recent research work has focused on specifying local heat transfer coefficients but overall thermal-hydraulic performance determines industrial applicability [12], [15]. In addition, some recent experimental studies on the shell-and-tube setup with counterflow indicate that it is essential to carefully balance the nanoparticle volume fraction and induced pressure drop for a positive net energy gain to be realized. Notwithstanding these developments, the exact basis for the distinction between parallel and counter flow operating limits at the laboratory-scale level, when using the  $\varepsilon$ -NTU approach and low concentration Al<sub>2</sub>O<sub>3</sub>-water suspensions, is still very sparse. This study conducts an experimental investigation of the performance of a shell-and-tube heat exchanger using an Al<sub>2</sub>O<sub>3</sub> water nanofluid at a low concentration (30g per 10 L). The effectiveness-NTU effective method is used to compare the thermal performance of the nanofluid with pure water in parallel flow and counter flow conditions. The current paper presents a realistic and systematic evaluation of nanofluid heat-transfer enhancement and thereby, establishing a basis on laboratory and teaching practice.

## 1. Experimental Setup and Methodology

### a) Experimental Apparatus

The present experimental investigation was performed by making use of a laboratory-based shell-and-tube heat exchanger. The reason behind choosing a shell-and tube design is its applicability in industrial settings, and multiple flow configurations can be accommodated. The exchanger consists of an outer shell and a tube bundle, thereby allowing the exchange of heat between two fluids that do not mix. In the configuration used herein, one of the fluids flows through the internal passage of the tubes while the counter-fluid flows in the shell. The outer shell is made of Pyrex and is 500 mm long with an inner diameter of 110 mm and an outer diameter of 120 mm. The tube bundle is made of eighteen copper tubes with an inner diameter of 6mm, an outer diameter of 6.2mm, and a length of 600mm. Three baffle spaces are incorporated in the bundle at 125 mm intervals. Fluid circulation is ensured by a pump that ensures continuous circulation through the exchanger. The volumetric flow rates of the two (hot and cold) streams are controlled by control valves and measured by flow meters located in the respective lines. Inlet and outlet temperatures of both fluids are measured with digital temperature sensors with a measurement range of 0 - 200 °C and multi-channel switching functionality. A data-logging device is used to capture data from the temperature and flow rate throughout the experiment. Connecting pipes and control plugs interconnect the parts and control both the fluid flow and the electrical supply to the system. The geometric characteristics and construction details of the heat exchanger components, such as the shell, the tube bundle, and the temperature indicator, are shown in Table 1. These dimensions define the physical geometry of the heat exchanger that is used throughout the experimental investigation and does not change under all test conditions.

**Table1. Geometric Specifications of the Shell-and-Tube Heat Exchanger Used in the Experiments**

Component	Parameter	Value	Unit
Shell	Length	500	mm
Shell	Inner diameter	110	mm
Shell	Outer diameter	120	mm
Tube	Inner diameter	6	mm
Tube	Outer diameter	6.2	mm
Tube	Length	600	mm
Tube bundle	Number of tubes	18	–
Tube bundle	Number of baffle spaces	3	–
Tube bundle	Distance between baffle spaces	125	mm
Component	Parameter	Value	Unit
Shell	Length	500	mm
Shell	Inner diameter	110	mm

The measurement and control instruments that are used to monitor the operating parameters of the system are shown in Table 2. These instruments include flow meters for regulating and measuring fluid flow rates, temperature sensors coupled with a digital temperature indicator to monitor inlet and outlet temperatures, and a data-logging apparatus for continuous data recording. Additional parts, such as the pump, heater, and control valves, account for the maintenance of constant operation and the availability of controllable experimental conditions in parallel-flow and counterflow configurations.

**Table2. Measurement Instruments Used in the Experimental Setup**

Instrument	Measured Parameter	Description	Location
Flow meter	Mass / volumetric flow rate	Used to measure the flow rate of hot and cold fluids	Installed in hot and cold fluid flow lines
Temperature sensors	Fluid temperature	Digital temperature sensors with multi-channel switching capability	Inlet and outlet of shell-and-tube sides
Temperature indicator	Temperature display	Digital temperature indicator with measurement range 0–200 °C	Connected to temperature sensors
Pump	Fluid circulation	Used to ensure continuous fluid flow through the heat exchanger	Hot fluid circulation loop
Data logging device	Data recording	Used to continuously record temperature and flow rate data	Connected to sensors and flow meters
Control valves	Flow regulation	Used to regulate fluid flow rates	Installed in hot and cold fluid lines
Heater	Heat input	Used to heat the water bath for hot fluid supply	Hot water circuit

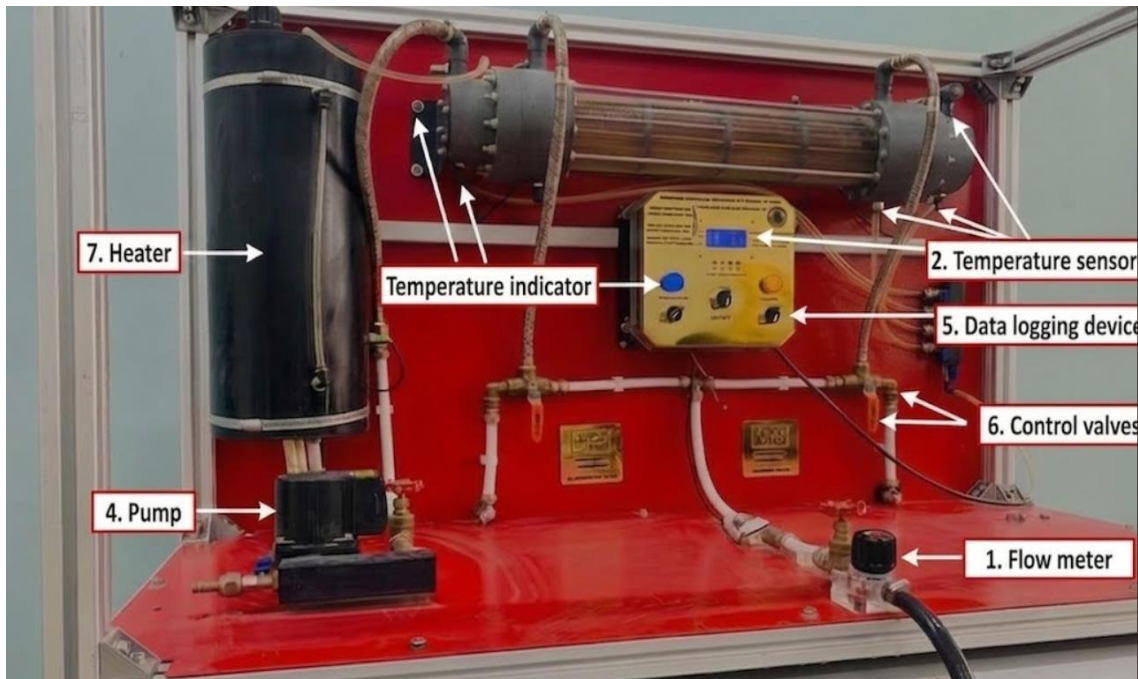


Figure 1. Experimental setup of the shell-and-tube heat exchange system.

### b) Nanofluid Preparation

The nanofluid was prepared in chemistry lab of Chemical Engineering Department, University of Misan using the standard two-step method. To achieve good thermal properties, the selection of aluminium oxide ( $Al_2O_3$ ) nanoparticles was made on the basis of rigorous scientific analysis. A high precision analytical balance was used to measure precisely 30g of  $Al_2O_3$  and the compound was added slowly up to the required concentration in 10 liters of deionized water. The suspension was first mechanically stirred continuously at [800 RPM] for [60 minutes] to disperse the particles and to break up any particle agglomerates to ensure homogeneous dispersion. After mechanical agitation the mixture was ultrasonicated (probe/bath solicitor) for (90 minutes) at (40 kHz). No other surfactant was used because they might also change the thermophysical properties of the base fluid. For each experiment, the nanofluid was prepared just before it was used to guarantee the maximum stability of the colloids.

### c) Experimental Procedure

Before each of the experimental runs, the shell-and-tube heat exchanger apparatus was prepared with the goal of obtaining reliable and repeatable measurements. The experimental setup was cleaned, and the water bath was about three-fourths full of demineralized water. All the drain valves were closed, and the system was checked for the absence of foreign particles in the configuration. The cold-water supply was attached to the cold-water flow meter line inlet, and the cold water from the shell side was drained. Initially, the heat exchanger was used in the counter-flow configuration. Before starting the system, all the ON/OFF switches of the control panel were checked to stay in the OFF position. The main power supply was then tested, and then the heater was turned on through the rotary switch on the control panel. The temperature of the water bath was set to the desired temperature using the digital temperature controller. The

flow control valve and bypass valve for the hot water circuit were opened, and the pump started to pump the hot fluid through the tubes. The flow control valve and the rotameter controlled the flow rate of hot water. After a sufficient period for the system to reach steady state conditions, the inlet and outlet temperatures of both the hot and cold fluids were measured. The experiment was repeated for different mass flow rates and inlet temperatures to assess thermal performance under different operating conditions. After finishing the counter-flow experiments, the same experimental protocol was run for the parallel-flow configuration. All measurements were recorded to be logged with the data logging device for later analysis.

#### d) Experimental Calculation

Experimental results collected from the shell-and-tube heat exchanger were used for analyzing the thermal performance of the heat exchanger under different operating conditions. The basic equations for the heat transfer rates, Logarithmic Mean Temperature Difference (LMTD) and effectiveness–NTU method were employed based on the well-known thermodynamic principles given. The heat transfer rate for the hot fluid was calculated using the following relation [16]:

$$Q_h = \dot{m}_h c p_h (T_{h,i} - T_{h,o}) \quad (1)$$

Similarly, the heat transfer rate for the cold fluid was determined by:

$$Q_c = \dot{m}_c c p_c (T_{c,i} - T_{c,o}) \quad (2)$$

To reduce the effect of experimental uncertainty, the average heat transfer rate was calculated by:

$$Q = \frac{Q_h + Q_c}{2} \quad (3)$$

The logarithmic mean temperature difference (LMTD) was calculated using the inlet and outlet temperatures of the hot and cold fluids according to the flow arrangement:

$$\Delta T_{lm} = \frac{\Delta T_1 - \Delta T_2}{\ln\left(\frac{\Delta T_1}{\Delta T_2}\right)} \quad (4)$$

Where

$$\Delta T_1 = T_{h,i} - T_{c,o}, \quad \Delta T_2 = T_{h,o} - T_{c,i}$$

The overall heat transfer coefficient was then determined using [17]:

$$U = \frac{Q}{A \Delta T_{lm}} \quad (5)$$

The total heat transfer area was calculated by:

$$A = \pi D L N \quad (6)$$

where  $D$  is the tube diameter,  $L$  is the length, and  $N$  is the number of tubes.

The effectiveness–NTU method was used to further assess the thermal performance of the heat exchanger. The effectiveness of the heat exchanger was evaluated using the effectiveness–NTU method and was defined by:

$$\varepsilon = \frac{Q}{Q_{max}} \quad (7)$$

The maximum possible heat transfer rate ( $Q_{max}$ ) was defined based on the minimum heat capacity rate of the two fluids:

$$Q_{max} = c_{\min}(T_{h,i} - T_{c,i}) \quad (8)$$

For the case where  $C_c < C_h$ , the maximum heat transfer rate was expressed as:

$$Q_{max} = c_c(T_{h,i} - T_{c,i}) \quad (9)$$

Similarly, for  $C_h < C_c$ , the maximum heat transfer rate was given by:

$$Q_{max} = c_h(T_{h,i} - T_{c,i}) \quad (10)$$

For a shell-and-tube heat exchanger, the effectiveness was evaluated using the standard  $\varepsilon$ -NTU relation[18]:

$$\varepsilon = \frac{2}{\left(1 + C_r + (1 + C_r^2)^{1/2} \left( \frac{(1 + \exp(-NTU(1 + C_r^2)^{1/2}))}{(1 - \exp(-NTU(1 + C_r^2)^{1/2}))} \right) - 1 \right)} \quad (11)$$

The number of transfer units (NTU) was assessed according to the formal definition defined in the theoretical framework. These computations were always performed for both pure water and Al<sub>2</sub>O<sub>3</sub> - water nanofluid, in parallel flow and counter flow configurations.

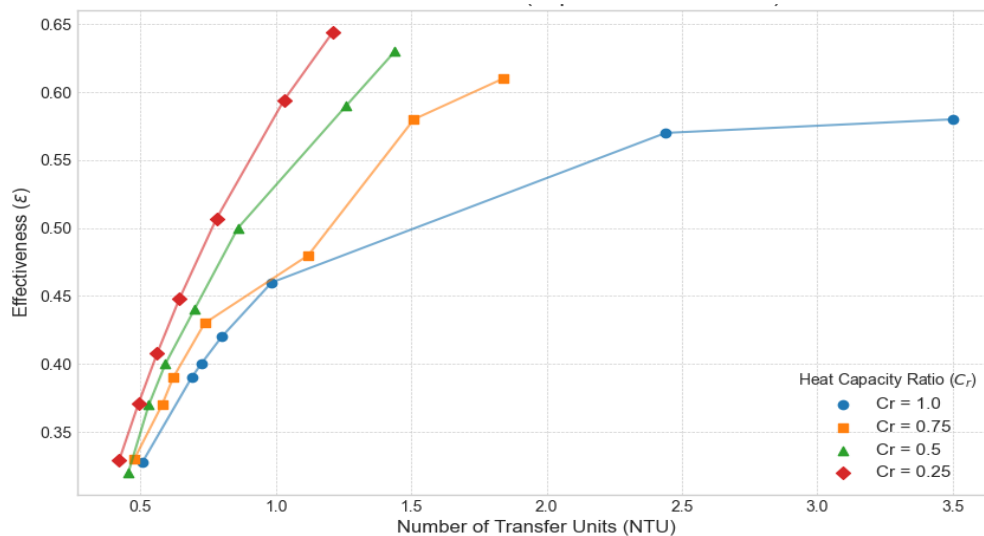
## 2. Results and discussion

### 3.1. Performance of the Heat Exchanger Using Water

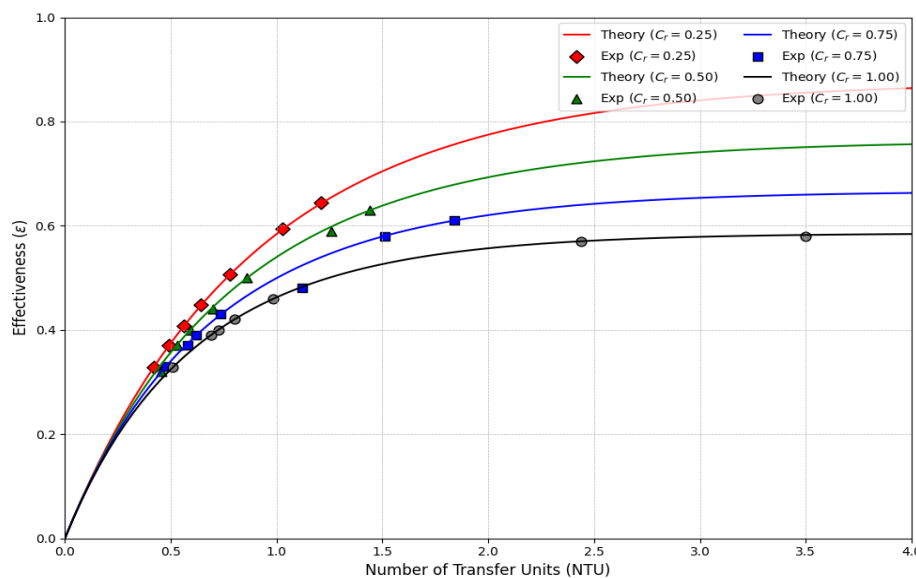
#### 3.1.1. Counter-Flow Arrangement

Figure 2 illustrates the effectiveness of a heat exchanger ( $\varepsilon$ ) which is dependent on the number of transfer units (NTU) at existing ratios of heat capacity between the working fluid and the heat exchange medium (water) ( $Cr = 0.25, 0.50, 0.75, \text{ and } 1.0$ ). The statistics clearly point to the fact that the effectiveness grows monotonically with NTU at all the heat capacity ratios considered, and thus, shows that the thermal performance of the counter-flow system is augmented by an increased overall heat transfer capability. As indicated in Figure 2, lower values of heat capacity ratios give maximum effect values at the same NTU values. Specifically, the highest level of effectiveness is observed in the scenario when  $Cr = 0.25$ , the least level of effectiveness is observed when  $Cr = 1.0$ . This tendency reflects the effect of heat capacity imbalance between the two fluids, with a lower minimum capacity rate allowing a greater fraction of the maximum heat transfer that is possible to be achieved. In the case of  $Cr=1.0$ , effectiveness decreases with the mass flow rate, and this can be explained by the fact that the residence time of the fluids in the exchanger is also low. Figure 3 confirms the data of experimental effectiveness NTU by comparing the experimental data with the theoretical effectiveness NTU curves of a shell-and-tube heat exchanger with one shell pass and two tube passes (TEMA E, 12 configuration). All the experimental measurements refer to the same trend and curvature as the theoretical ones of all the considered ratios of the heat capacities, which confirms the accuracy of the experiments and the validity of the effectiveness NTU methodology used. There are small differences in experimental and theoretical findings that can be noticed,

particularly when the NTU is high. These anomalies can be explained by experimental uncertainties and heat losses that are inevitable to the surrounding environment, which the theoretical perfect model fails to explain. Overall, the evidence shows that the counterflow configuration provides good thermal operation and that the laboratory design can reproduce the expected behavior of the heat-transfer.



**Figure 2. Experimental effectiveness ( $\epsilon$ ) plotted against Number of Transfer Units (NTU) for varying heat capacity ratios ( $C_r = 0.25, 0.50, 0.75, 1.0$ ).**



**Figure 3. Validation of experimental results: comparison of experimental effectiveness ( $\epsilon$ ) against the theoretical effectiveness-NTU curves for a shell-and-tube heat exchanger with one shell pass and two tube passes (TEMA E, 1-2 configuration).**

### 3.1.2. Parallel-Flow Arrangement

Figure 4 shows the dependence of heat exchanger effectiveness ( $\epsilon$ ) on number of transfer units (NTU) for the parallel flow configuration using water as the working fluid over a range of heat capacity ratios ( $Cr = 0.25, 0.50, 0.75$  and  $1.0$ ). The data show that effectiveness increases at a rapid rate at low NTU values and asymptotically approaches a limiting value as NTU increases. This trend is typical of parallel-flow heat exchangers in which the maximum temperature difference between the hot and cold streams is at a point close to the inlet point and decreases dramatically along the flow passage. As can be seen in Figure 4, effectiveness decreases with a higher heat capacity ratio at a given NTU. The superior effectiveness values are seen for  $Cr = 0.25$  while the inferior values relate to  $Cr = 1.0$ . This observation is consistent with the reduced thermal driving potential that is related to high heat capacity ratios. For all investigated cases the effectiveness values of the parallel-flow arrangement are still inferior to the effectiveness values obtained for the counter-flow configuration under comparable NTU conditions. The comparison between experimental data points and theoretical effectiveness–NTU curves in Figure 4 shows good agreement in terms of both trends and magnitudes. Experimental observations closely follow theoretical predictions over the entire NTU spectrum, thus also verifying the correctness of the empirical measurements and the applicability of the effectiveness-NTU methodology. Minor differences observed at higher NTU values can be attributed to experimental errors and unavoidable heat losses which are not included in the ideal theoretical model. In summary, the results indicate that, despite the augmentation of the mass flow rates, which enhances, despite the heat transfer rate, the parallel flow configuration shows lower effectiveness due to the rapid attenuation of the temperature difference along the exchanger length. This inherent limitation is the reason for the relatively poor thermal performance of the parallel flow operation compared to the counter-flow configuration.

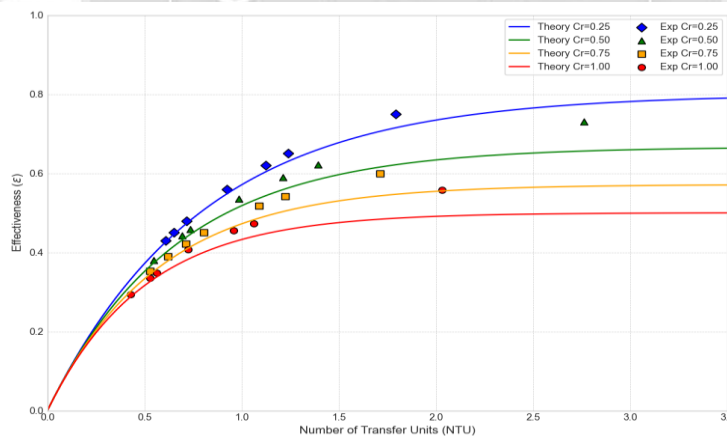


**Figure 4. Comparison of experimental data with theoretical effectiveness-NTU curves for a parallel-flow heat exchanger, demonstrating asymptotic behavior at high NTU values.**

### 3.3. Performance of the Heat Exchanger Using Nanofluid

#### 3.3.1. Counter-Flow Arrangement with Nanofluid

Figure 5 shows the dependence of the overall heat transfer coefficient, ( $U$ ), on the mass flow rate of the hot fluid for both pure water and  $Al_2O_3$ - water nanofluid in a counter-flow configuration. In the latter case,  $U$  increases with increasing mass flow rate, indicating an enhanced convective heat transfer caused by increasing fluid velocities. For all the mass flow rates examined, the  $Al_2O_3$ -water nanofluid always shows higher  $U$  values compared to the pure water. The difference between the two data sets is clear at every point in the entire operating range, indicating that there is a systematic enhancement of the thermal performance due to the nanofluid. The augmentation is strongest at moderate to high mass flow rates where the nanofluid maintains a superior overall heat transfer coefficient whereas the pure water system has a comparatively subdued increase. The shaded region in Figure 5 represents the enhanced heat transfer capacity achieved using nanofluid. This gain can be considered as a reduction of tube side thermal resistance and hence facilitating more efficient heat exchange between the hot and cold streams in counter flow operation. The constant divergence between the nanofluid and the water curves show that the observed enhancement is not limited to a small range of operations, but in fact is applicable for all conditions considered in the evaluation. In conclusion, the data shows that adding  $Al_2O_3$ -water nanofluid on tube side of counter flow heat exchanger causes a quantifiable and sustained increase in the overall heat transfer coefficient compared to pure water. This finding provides evidence for the effectiveness of nanofluid application for improving the performance in shell-and-tube exchangers without the need for a change in the geometry of the heat exchanger.

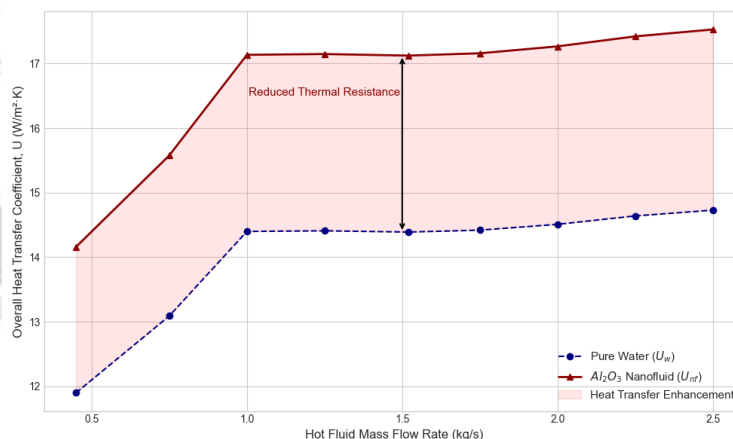


**Figure 5. Variation of the overall heat transfer coefficient ( $U$ ) with mass flow rate for pure water and  $Al_2O_3$  nanofluid. The shaded region represents the enhancement in heat transfer capacity due to the reduction in tube-side thermal resistance.**

### 3.3.2. Parallel-Flow Arrangement with Nanofluid

Figure 6 shows the relation between effectiveness of the heat exchanger ( $\epsilon$ ) and mass flow rate for parallel flow configuration using either pure water or Al<sub>2</sub>O<sub>3</sub>-Water nanofluid. The mass flow rate values in both cases increase monotonically with increasing values of  $\epsilon$ , which indicates improved heat transfer efficiency due to high convective transport. Across the entire spectrum of mass-flow rates tested, the Al<sub>2</sub>O<sub>3</sub> water nanofluid can achieve greater effectiveness than pure water at all mass-flow rates. The difference between the two curves remains the same throughout the operating range, which is a proof of uniform augmentation of thermal performance when the nanofluid is used. Figure 6 further quantifies this advantage, with an increase in effectiveness of about 15-16% compared to pure water under the same operating conditions. Nevertheless, the effectiveness of the parallel flow configuration is still inferior to the effectiveness that has been reported for the counter flow arrangement. This observation is in line with the inherent characteristics of parallel-flow heat exchangers, where the temperature difference between the hot and the cold stream is greatest around the inlet with a rapid decrease downstream. Accordingly, although the use of Al<sub>2</sub>O<sub>3</sub>-water nanofluid can improve the thermal performance of the parallel flow exchanger, the physical limitations of the parallel flow configuration restrict the effectiveness that can be achieved as compared to counter flow operation. In summary, the results strengthen that the usage of a nanofluid increases the effectiveness of a parallel flow heat exchanger. However, the results also highlight that maximum performance improvements are achieved when nanofluids utilization is combined with a better flow arrangement.

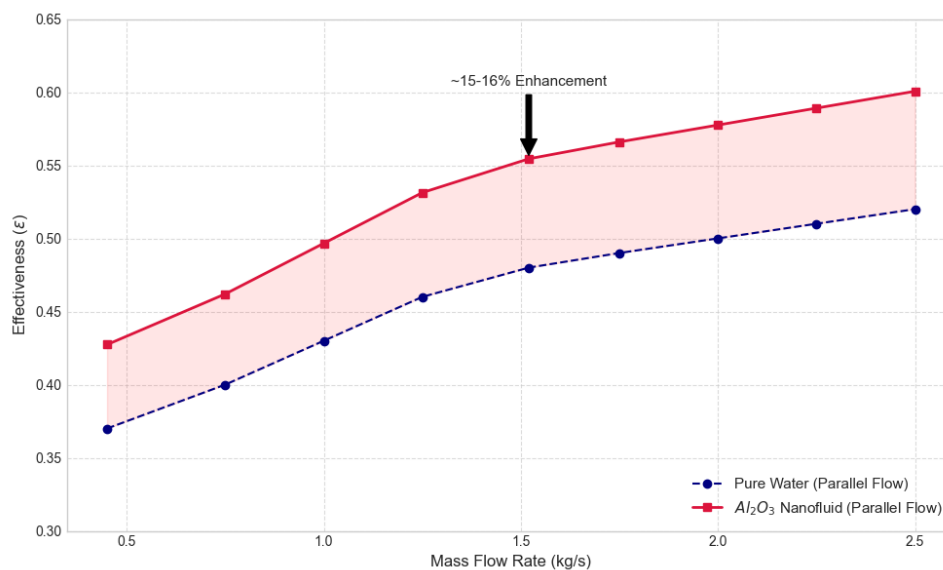


**Figure 6. Comparative effectiveness of the parallel-flow heat exchanger arrangement operating with pure water and Al<sub>2</sub>O<sub>3</sub> nanofluid**

### 3.4. Comparative Discussion

This direct comparison of water and nanofluid operation is an indication of the positive contributions of Al<sub>2</sub>O<sub>3</sub> nanoparticles to the thermal characteristics of the shell-and-tube heat exchanger. For both flow arrangements, the nanofluid improves the temperature difference, rate of heat transfer, and effectiveness. The counter-flow configuration in both cases offers higher effectiveness than the parallel-flow configuration for both working fluids. The observed performance enhancement by using the nanofluid is more pronounced in the counter flow arrangement because of the larger effective temperature difference along the heat exchanger length. Overall, the experimental results show that the substitution of pure water with Al<sub>2</sub>O<sub>3</sub>-nanofluid water results in a measurable performance increase of the heat exchanger without any changes in the geometry and principle of operation.

### 5. Conclusions

This study examined the thermal performance of a shell-and-tube heat exchanger with pure water and Al<sub>2</sub>O<sub>3</sub> and water nanofluid in a parallel flow and counter flow heat exchanger in an experimental manner. The main conclusions, as supported by the experimental results, are summarized as follows:

1. As shown in Figure 7, the counter-flow configuration always results in higher effectiveness than a parallel-flow arrangement for both pure water and nanofluid in the whole mass flow rate range investigated, hence confirming the better thermal performance of counter-flow operation.
2. The use of Al<sub>2</sub>O<sub>3</sub>-water nanofluid results in a good increase in the effectiveness of the heat exchanger compared to that of pure water for all the flow configurations. The average effectiveness comparison represented in Figure 9 reveals an improvement of around 15-16% for parallel-flow operation and 17-19% for counter-flow operations.
3. The effectiveness grows with the increase of mass flow rate for both working fluids, as shown in Figure 1, and the separation between the nanofluid and water curves is obvious at all operating conditions, which shows the consistency of the improvement of performance for the nanofluid.
4. The overall heat transfer coefficient increases monotonously with mass flow rate in both cases of pure water and nanofluid as shown in Figure 8. Higher values obtained using the nanofluid are indicative of a decrease in thermal resistance on the tube side and an increase of the convective heat transfer behavior.
5. Despite the improvement in effectiveness obtained using nanofluid in parallel flow configuration, the effectiveness values are far less than those obtained in the counterflow configuration, as can be seen from the comparative trends presented in Figures 7 and 9. This limitation is attributed to the inherent temperature distribution characteristics of parallel flow heat exchangers.
6. The combination of the interpretations of Figures 7-9 shows that the best thermal performances are achieved when nanofluid application is combined with counter-flow

operation in terms of simultaneously optimizing the working fluid selection and flow arrangement.

Overall, the experimental results prove that Al<sub>2</sub>O<sub>3</sub>-Water nanofluid is an effective working fluid for improving the thermal performance of heat exchangers (shell-and-tube) without any geometric change, and optimum working conditions are obtained by counter-flow conditions.

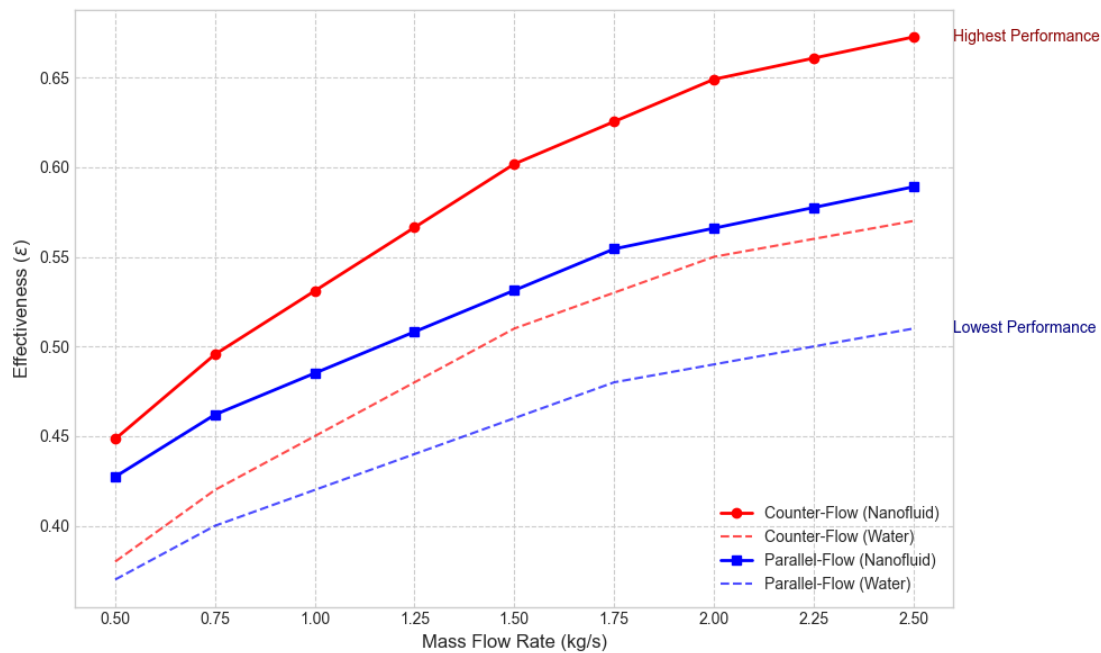


**Figure 7. Comparison of thermal effectiveness ( $\epsilon$ ) across all experimental configurations. The data highlights that the **counter-flow nanofluid** arrangement yields superior thermal performance, confirming that optimal results require both the correct fluid choice and flow geometry.**

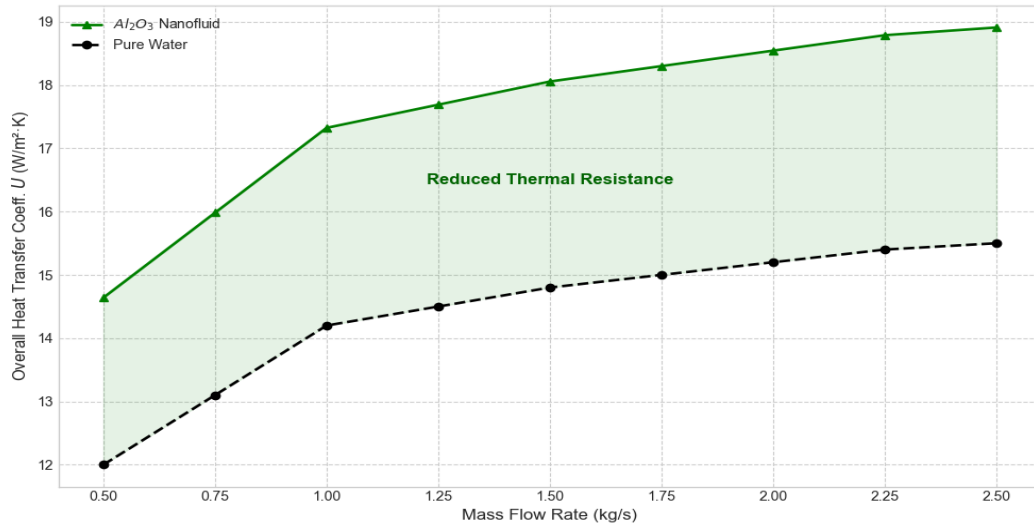


Figure 8. shows the variation of the overall heat transfer coefficient (U) against the mass flow rate. Nanofluid has consistently high values of U which reflects the capability of the addition of Al<sub>2</sub>O<sub>3</sub> nanoparticles to reduce the thermal resistance at the tubular side and to increase the convective heat transfer.

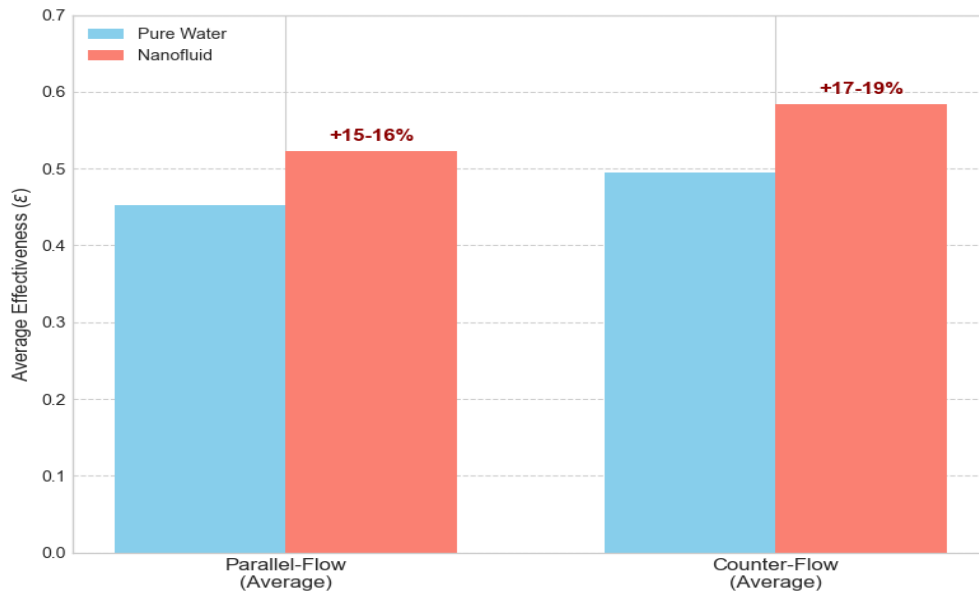


Figure 9. Summary of the average thermal effectiveness strengthening. The application of **Al<sub>2</sub>O<sub>3</sub>-based** nanofluid resulted in a 17-19% increase in the thermal effectiveness under counter flow condition and 15-16% increase under parallel flow condition as compared to pure water.

Nomenclature  
**Roman Symbols**

Symbol	Description	Unit
$A$	Heat transfer area	$m^2$
$C$	Heat capacity rate ( $C = \dot{m}c_p$ )	$W \cdot K^{-1}$
$C_c$	Cold fluid heat capacity rate	$W \cdot K^{-1}$
$C_h$	Hot fluid heat capacity rate	$W \cdot K^{-1}$
$C_r$	Heat capacity ratio ( $C_{min}/C_{max}$ )	–
$C_p$	Specific heat capacity	$J \cdot kg^{-1} \cdot K^{-1}$
$D$	Tube diameter	m
$L$	Tube length	m
$\dot{m}$	Mass flow rate	$kg \cdot s^{-1}$
$NTU$	Number of transfer units	–
$Q$	Heat transfer rate	W
$Q_{max}$	Maximum possible heat transfer rate	W
$T$	Temperature	K
$U$	Overall heat transfer coefficient	$W \cdot m^{-2} \cdot K^{-1}$
$\Delta T_{lm}$	Log means temperature difference	K

**Greek Symbols**

Symbol	Description	Unit
$\varepsilon$	Heat exchanger effectiveness	–
$\mu$	Dynamic viscosity	Pa·s
$\rho$	Density	$kg \cdot m^{-3}$

Subscript	Description
$c$	Cold fluid
$h$	Hot fluid
$i$	Inlet
$o$	Outlet
$min$	Minimum value
$max$	Maximum value
$nf$	Nanofluid
$w$	Pure water

**Reference**

- [1] Mitcoe, & Diat, and A. Pune, “International Journal of Current Engineering and Technology A Review on Use of nanofluids for heat exchangers,” 2017. [Online]. Available: <http://inpressco.com/category/ijcet>
- [2] C. T. Nguyen *et al.*, “Viscosity data for Al<sub>2</sub>O<sub>3</sub>–water nanofluid—hysteresis: is heat transfer enhancement using nanofluids reliable?,” *International Journal of Thermal Sciences*, vol. 47, no. 2, pp. 103–111, Feb. 2008, doi: 10.1016/J.IJTHEMALSCI.2007.01.033.
- [3] S. U. S. Choi and J. A. Eastman, “Enhancing thermal conductivity of fluids with nanoparticles,” in *Proceedings of the ASME International Mechanical Engineering Congress and Exposition*, San Francisco, USA, 1995.

- [4] J. A. Eastman, S. R. Phillpot, S. U. S. Choi, and P. Keblinski, "Thermal transport in nanofluids," *Annu. Rev. Mater. Res.*, vol. 34, pp. 219–246, 2004.
- [5] X. Q. Wang and A. S. Mujumdar, "Heat transfer characteristics of nanofluids: A review," *International Journal of Thermal Sciences*, vol. 46, pp. 1–19, 2007.
- [6] R. Subramanian, A. Senthil Kumar, K. Vinayagar, and C. Muthusamy, "Experimental analyses on heat transfer performance of TiO<sub>2</sub>–water nanofluid in double-pipe counter-flow heat exchanger for various flow regimes," *Journal of Thermal Analysis and Calorimetry 2019 140:2*, vol. 140, no. 2, pp. 603–612, Oct. 2019, doi: 10.1007/S10973-019-08887-1.
- [7] N. Bozorgan and M. Shafahi, "Numerical investigation of Al<sub>2</sub>O<sub>3</sub>–water nanofluid in a plate heat exchanger," *Appl. Therm. Eng.*, vol. 121, pp. 131–141, 2017.
- [8] A. Sözen, A. Khanlari, and E. Çiftçi, "Experimental investigation of nanofluid usage in a plate heat exchanger," *International Journal of Renewable Energy Development*, vol. 8, no. 1, pp. 27–32, 2019.
- [9] A. M. Hassaan, "Evaluation of heat transfer performance using MWCNT nanofluids in a double-pipe heat exchanger," *Proceedings of the Institution of Mechanical Engineers, Part E*, vol. 236, no. 5, pp. 2139–2146, 2022.
- [10] I. M. Shahrul, I. M. Mahbulbul, R. Saidur, and M. F. M. Sabri, "Experimental investigation on Al<sub>2</sub>O<sub>3</sub>–W, SiO<sub>2</sub>–W and ZnO–W nanofluids and their application in a shell and tube heat exchanger," *Int. J. Heat Mass Transf.*, vol. 97, pp. 547–558, Jun. 2016, doi: 10.1016/J.IJHEATMASSTRANSFER.2016.02.016.
- [11] B. Farajollahi, S. G. Etemad, and M. Hojjat, "Heat transfer of nanofluids in a shell and tube heat exchanger," *Int. J. Heat Mass Transf.*, vol. 53, no. 1–3, pp. 12–17, Jan. 2010, doi: 10.1016/J.IJHEATMASSTRANSFER.2009.10.019.
- [12] S. M. Hasan, S. Iqbal, I. Khan, A. Javaid, and M. Sajid, "Performance enhancement of a shell-and-tube heat exchanger using a novel baffle design," *Case Studies in Thermal Engineering*, vol. 74, p. 106800, Oct. 2025, doi: 10.1016/j.csite.2025.106800.
- [13] G. Gao, Z. Feng, Y. Cai, T. Luo, M. SONG, and X. Zhu, "Numerical Analysis of Full-Scale Multi-Path Shell-and-Tube Heat Exchangers with Corrugated Tubes," 2024, doi: 10.2139/SSRN.4978515.
- [14] M. Ünverdi and H. Küçük, "Energy conversion efficiency of nanofluids in mini-channel shell-and-tube heat exchangers," *Case Studies in Thermal Engineering*, vol. 71, 2025.
- [15] G. Gao, Z. Feng, Y. Cai, T. Luo, M. Song, and X. Zhu, "Numerical Analysis of Full-Scale Multi-Path Shell-and-Tube Heat Exchangers with Corrugated Tubes." [Online]. Available: <https://ssrn.com/abstract=4978515>
- [16] Y. A. Çengel and A. J. Ghajar, *Heat and Mass Transfer: Fundamentals and Applications*. McGraw-Hill Education, 2020. [Online]. Available: <https://www.mheducation.com/highered/product/heat-and-mass-transfer-fundamentals-and-applications-cengel.html?viewOption=student>

## دراسة تجريبية لأداء مبادل حراري من النوع القشري والأنبوبي باستخدام مائع نانوي من أكسيد الألمنيوم والماء

الحسين علي خلف

شركة نفط ميسان، العراق، العمارة

[alhussen2009mh@gmail.com](mailto:alhussen2009mh@gmail.com)

### الخلاصة

تقدم هذه الورقة البحثية دراسة مقارنة للخواص الحرارية لمبادل حراري من النوع القشري والأنبوبي (Shell and tube) المملوء بمائع نانوي مكون من أكسيد الألمنيوم والماء ( $Al_2O_3$ ) ، مقارنة بمبادل آخر ممزوج بالماء النقي فقط. وقد تقرر استخدام أكسيد الألمنيوم ( $Al_2O_3$ ) نظراً لاستقراره الكيميائي، وتوفره تجارياً، وثبوت فاعليته في تحسين الموصلية الحرارية دون التسبب في أضرار هيدروليكية بالغة. أجريت التجارب على نطاق من أرقام رينولدز (Reynolds numbers) يتراوح بين 12,600 إلى 63,300، وبتركيز بلغ 30 غراماً لكل 10 لترات من المائع الأساسي. واستخدم أسلوب الفاعلية وعدد وحدات النقل (NTU) لمعالجة وتحليل البيانات. تشير النتائج إلى أن تصميم التدفق المتعكس (Counter-flow) حقق تأثيراً إيجابياً كبيراً، حيث أدى إلى زيادة الفاعلية بنسبة تتراوح بين 17% و 19%، وخفض درجة حرارة المائع عند الحد الأقصى بنحو 5 درجات مئوية. كما أدى تكوين التدفق المتوازي (Parallel-flow) إلى تعزيز الأداء أيضاً، مع زيادة تقريبية في الفاعلية بلغت 16%. وعلى الرغم من تحقيق التحسن في الموصلية الحرارية نتيجة إضافة الجسيمات النانوية، إلا أن الزيادة المصاحبة في لزوجة المائع تعني أن الأمر قد يتطلب طاقة ضخ إضافية (Pumping power) وختاماً، فإن الموائع النانوية ذات التركيزات المنخفضة من أكسيد الألمنيوم ( $Al_2O_3$ ) تعد مفيدة ومبشرة لتعزيز الكفاءة الحرارية لعمليات انتقال الحرارة المستخدمة في الصناعة، شريطة الحد من الخسائر الهيدروليكية بشكل كافٍ. الكلمات الدالة: مبادل حراري قشري وأنبوبي؛ مائع نانوي؛ تعزيز انتقال الحرارة؛ طريقة الفاعلية وعدد وحدات النقل (NTU)؛ ترتيب التدفق المتعكس.